Journal of Southeast University (English Edition) Vol. 22, No. 2, pp. 208 – 212 June 2006 ISSN 1003—7985

PSO algorithm for Young's modulus reconstruction

Chen Min Wang Nan Tang Wencheng

(College of Mechanical Engineering, Southeast University, Nanjing 210096, China)

Abstract: To get the quantitive value of abnormal biological tissues, an inverse algorithm about the Young's modulus based on the boundary extraction and the image registration technologies is proposed. With the known displacements of boundary tissues and the force distribution, the Young's modulus is calculated by constructing the unit system and the inverse finite element method (IFEM). Then a tough range of the modulus for the whole tissue is estimated referring the value obtained before. The improved particle swarm optimizer (PSO) method is adopted to calculate the whole Yong's modulus distribution. The presented algorithm overcomes some limitations in other Young's modulus reconstruction methods and relaxes the displacements and force boundary condition requirements. The repetitious numerical simulation shows that errors in boundary displacement are not very sensitive to the estimation of next process; a final feasible solution is obtained by the improved PSO method which is close to the theoretical values obtained during searching in an extensive range.

Key words: Young's modulus; inverse finite element method; particle swarm optimizer

The abnormalities of biological tissues always induce changes in the elastic properties which are useful in diagnosing diseases. The physical palpation, an old effective diagnostic way, is a restricted method to measure abnormal tissues in deep bodies. With the development of medical imaging, more and more technologies are used in measuring abnormalities of tissues. Currently, the Young's modulus reconstruction for soft tissues is grounded on ultrasonic imaging technology. There are mainly two methods: the vibration sonoelastography and the static compression technique for displacement estimation.

Vibration sonoelastography techniques obtain the Young's modulus distribution by analyzing reflected wave velocities and damping. In other words, low frequency mechanical vibrations, which can cause tissue co-frequency, are applied on the surface of tissues, and then the reflected shear wave velocities or the tissue vibration velocities, related to the tissue viscoelasticity, were measured to obtain the Young's modulus[1-3]. The static compression technique for displacement estimation is another important method to measure tissue's Young's modulus. Static pressure is loaded on the surface of tissues, which can produce stress of tissues and changes of ultrasonic echoes. By analyzing ultrasonic echoes, the displacement distribution was measured, and then the relative tissue's Young's modulus distribution was obtained using the inverse method[4-7]. Zhu et al.[8] proposed the FEA-based modulus estimation technique, assuming all the displacement distribution as a known condition. Under the same condition, Liew et al.[9] estimated the modulus distribution using the B-spline and the gradient method.

However, these methods have essential disadvantages. Vibration sonoelastography is the point by point scanning, so the efficiency is low. Furthermore, its images just half-quantitatively show the mechanical properties. Static compression technique for displacement estimation is composed of the coherence technique and the incoherent technique. Today, the speckle tracking technology is used more widely, while it is too sensitive to the coherence of fore-and-aft compression. Hence, it is just used in small loads commonly.

With the high speed development of imaging, the boundaries of tissues and lesions can be taken out, effectively based on CT[10], MRI[11] and ultrasonic imaging[12]. Then by means of image registration[13], we can get the boundary displacements. And we sincerely hope to find a new method to estimate the quantitative Young's modulus distribution with loose conditions. The details of our modulus estimation method will be described below.

1 Algorithm for Young's Modulus Reconstruction

The Young's modulus reconstruction method is proposed in this chapter. The flowchart of the algorithm is shown in Fig. 1.

Received 2005-12-14.

Biographies: Chen Min (1981—), female, graduate; Tang Wencheng (corresponding author), male, doctor, professor, tangwc@seu.edu.cn.

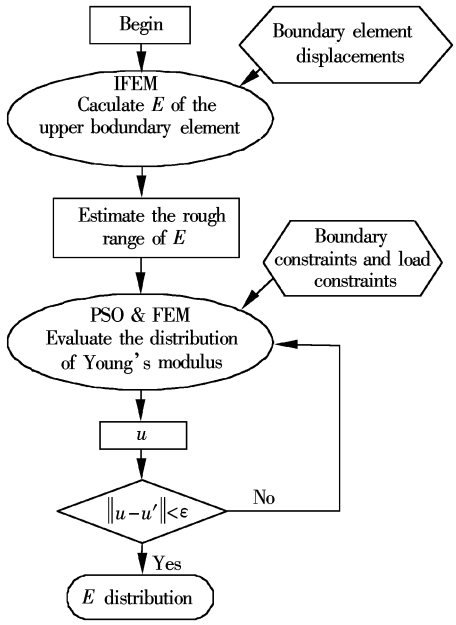

Fig. 1 Flowchart of the Young's modulus reconstruction

1.1 Inverse finite element method (IFEM)

The formula of the finite element method is founded on the variation principle of elastic mechanics. For the 2-D problems, the common choices for element types are triangles and quadrilaterals. Here, we take the quadrilateral element as an example.

Each element matrix equation for elasticity problems has the form

$$\boldsymbol{K}^{e}\boldsymbol{\delta}^{e}=\boldsymbol{f}^{e} \tag{1}$$

where $\boldsymbol{K}^{e}$, $\boldsymbol{\delta}^{e}$ and $\boldsymbol{f}^{e}$ are the element stiffness matrix, the element nodal displacement vector and the element nodal force, respectively.

A contiguous area in the abnormal domain can be meshed into numbers of elements, which are rectangles of the same size in this paper. The matrix equation of the whole meshed area has the form

$$\boldsymbol{K}\boldsymbol{\delta}=\boldsymbol{f} \tag{2}$$

where $\boldsymbol{K}$ is the global stiffness matrix, $\boldsymbol{\delta}$ is the global nodal displacement vector, and $\boldsymbol{f}$ is the global nodal force vector. Each component of $\boldsymbol{K}^{e}$ is accumulated onto $\boldsymbol{K}$. Hence, each component of the global stiffness matrix is a linear combination of the Young's modulus of each element. So $\boldsymbol{K}$ can be written as

$$\boldsymbol{K}=[K_{ij}] \qquad i=1,2,\ldots,N;j=1,2,\ldots,N \tag{3}$$

$$[K_{ij}]=\sum_{e=1}^{Ne}c_{e}^{ij}E^{e} \tag{4}$$

where c_{e}^{ij} are the constants, and E^{e} is the element Young's modulus.

The traditional finite element problem is to solve $\boldsymbol{\delta}$ with $\boldsymbol{K}$, and $\boldsymbol{f}$ is already known. The inverse FEM is to solve $\boldsymbol{K}$ or $\boldsymbol{f}$. In our research, we reconstruct the Young's modulus (E) with the boundary displacements and the outside forces already known.

1.2 Particle swarm optimizer (PSO) algorithm

The PSO[14], one kind of swarm intelligence, is proposed by Kennedy and Eberhart in 1995. It is similar to the genetic algorithm where the system is initialized with a population of random solutions. However, it does not have the process of chiasms and variations, so its advantages are the background of intelligence and the simple operation.

The updated velocity is influenced by the global best particle and the local best particle position.

$$V=wV+c_1r_1(P_{\text{best}}-P_{\text{present}})+c_2r_2(g_{\text{best}}-P_{\text{present}}) \tag{5}$$

$$P_{\text{present}}=P_{\text{present}}+V \tag{6}$$

where c_1 and c_2 are the study factors and usually $c_1=c_2=2$; r_1 and r_2 are the random numbers between 0 and 1; P_{best}, g_{best} and P_{position} are the local best particle position, global best particle position and present particle position in the swarm, respectively; w is the inertia weight. By Eqs. (5) and 6) and iterations of the evolution, the PSO can converge to the best solution.

As w concerned, Shi et al.[15] put forward a linearly decreasing weight (LDW) strategy,

$$w(t)=\frac{(w_{\text{ini}}-w_{\text{end}})(T_{\max}-t)}{T_{\max}+w_{\text{end}}} \tag{7}$$

where t is the current iteration times; $T_{\max}$ is the maximum evolution generation; w_{ini} and w_{end} are the initial inertia weight and the finial inertia weight, respectively. Comparatively, when w is in a large value, the global search ability is better, or it is the local search ability.

2 Evaluating Young's Modulus Based on IFEM and PSO

For biological tissues we can get the boundary displacements based on the technologies of boundary extraction and image registration. With the additional boundary conditions, the Young's modulus of the upper boundary elements is calculated by the IFEM, then its distribution within the whole area using the PSO is evaluated. The initial value and the searching range of particles referred to the value E calculated before. The reconstruction of the Young's modulus is shown in Fig. 1.

2.1 Calculating E using IFEM

As shown in Fig. 2, we take the upper limit elements from the whole system, where i denotes the number of elements, f is the force applied on nodes and the black dots represent the inner nodes.

With the assumption that the displacements of

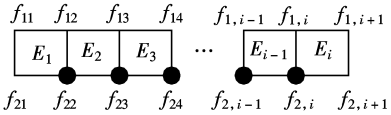

Fig. 2 Upper boundary elements

outside elements are known, while the Young's modulus of each element is unknown, take two elements as a small unit, for example E_1 and E_2. The details of these steps are provided below.

Step 1 The variables for the small unit are E_1, $E_2, f_{21x}, f_{21y}, f_{22x}, f_{22y}, f_{23x}, f_{23y}, u_{22}$, v_{22}, u_{23} and v_{23}. Assume that $f_{13x} = 0$, $f_{13y} = 0.5f_{13}$. And f_{ij} is the nodal force, u_{ij} is the x-directional displacement and v_{ij} is the y-directional displacement of the node ij.

Step 2 Calculate E_1 and E_2 using the IFEM.

Step 3 Make E_1 as a known variable, then calculate u_{22}, v_{22}, f_{12x} and f_{12y}, which are used as known variables in the next step.

Step 4 Update the new small unit and repeat step 2 and step 3. Then we can get p_{13x}, p_{13y}.

Step 5 If $|p_{13x} - f_{13x}| < \varepsilon$, $|p_{13y} - f_{13y}| < \varepsilon$, continue the next unit, or go back to step 1 with $f_{13x} = p_{13x}$ and $f_{13y} = p_{13y}$.

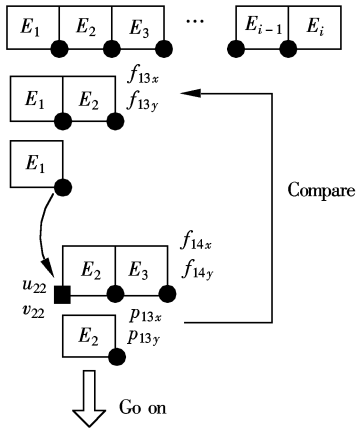

Fig. 3 Sketch map for calculating E

Then why do we take two elements as a small unit? With the assumption that f_{13x} and f_{13y} are known, there are 12 equations as well as 12 variables in the unit. Meanwhile, f_{13x} and f_{13y} will affect the precision of the first element less.

2.2 Calculating global E distribution using PSO

According to the Young's modulus calculated above, we can give a tough estimation of the whole domain. Define optimization fitness function as P,

$$P = \left| \frac{u' - u}{u} \right| \times 100\% \tag{8}$$

where u' is the calculated boundary nodal displacement, and u is the measured nodal displacement.

Step 1 Take $\{E_i\}$ $(i = 1, 2, \ldots, N)$ as the particles. Initialize these particles and the velocities.

Step 2 Calculate fitness value, and update the best fitness value.

Step 3 Calculate particle velocity according to Eq. (5), and update the particle position according to Eq. (6).

Step 4 If the maximum iterations or the minimum error criteria is not attained, jump to step 2, or end.

In the numerical simulation, we use one group of particles and three groups of particles to solve the E distribution respectively.

3 Test Example

3.1 Model

We simulate an object for which the forward approach solves. The dimension of the simulated object is 4×4. The Young's modulus of the background is 20 kPa which approximates the stiffness of normal glandular breast tissue[8]. There are two targets in the object that simulate the abnormal tissues, one is 45 kPa and the other is 10 kPa. And the softest tissues and tissue-like materials (with the exception of the lung) can be considered incompressible, so we assume the Poisson ratio is 0.49. And the displacements of boundary nodes are already known by the measurements.

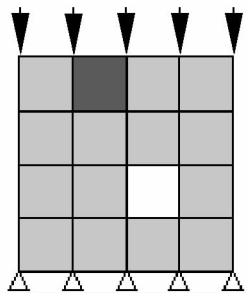

Fig. 4 Test model

3.2 Results

If the measured boundary nodal displacements are accurate, the Young's modulus of upper boundary elements are shown in Tab. 1.

Tab. 1 Numerical results with ideal input

Item	Theoretical value/kPa	Calculated value/kPa	Relative error/%
E_1	20	19.97	0.15
E_2	45	44.35	1.44
E_3	20	19.89	0.55
E_4	20	19.92	0.40

Final optimization results of the algorithm are shown in Tab. 2. In the test, all the algorithms run dozens of times with 50 iterations.

Tab. 2 Young's distribution

No.	Theoretical value/kPa	Calculated value/kPa	Relative error/%
1	20.00	20.05	0.25
2	20.00	19.42	2.90
3	20.00	19.67	1.65
4	20.00	18.52	7.40
5	20.00	18.38	8.10
6	20.00	20.44	2.20
7	10.00	11.97	19.70
8	20.00	19.78	1.10
9	20.00	19.73	1.35
10	20.00	18.75	6.25
11	20.00	18.19	9.05
12	20.00	19.58	2.10
13	20.00	19.97	0.15
14	45.00	44.35	1.44
15	20.00	19.89	0.55
16	20.00	19.92	0.40

Inevitably, there is noise on the displacement estimates that are used in modulus estimation. So it is necessary to study the effect of noise on the input data in the results. We rely on numerical simulation again. 10% deviations of the theoretical displacements are used to study the relationship between the noise power and the modulus estimation error.

Tab. 3 Numerical results with noisy input

Item	Theoretical value/kPa	Calculated value/kPa	Relative error/%
E_1	20.00	18.15	9.25
E_2	45.00	40.31	10.42
E_3	20.00	18.08	9.60
E_4	20.00	18.11	9.45

Comparing Tab. 1 and Tab. 3, we find that the errors in boundary displacement are not very sensitive to the estimation of the next process.

4 Conclusions

The method proposed in this paper is based on the technologies of image registration and boundary extraction. Through a series of research results, we find that:

1) The Young's modulus of the lesions can always be close to the theoretical values searching in an extensive range. It is of great significance to the application.

2) This mathematical model has not a unique solution essentially. However, it can produce a good feasible solution, even under noisy displacement input.

And compared with other algorithms for the Young's modulus reconstruction, the proposed method requires loose requirements. Meanwhile, the technology of image registration can be applied on the technologies of CT, MRI and ultrasonic imaging, the model can be used widely, and has the advantage of expandability. How to advance the accuracy of the results by inducing other optimization methods and how to make our method be applied in practice are future research for us.

References

[1] Catheline S, Thomas J L, Wu F, et al. Diffraction field of a low frequency vibrator in soft tissues using transient elastography [J]. *Ultrasonics, Ferroelectrics and Frequency Control*, 1999, **46**(4): 1013 − 1019.

[2] Sandrin L, Tanter M, Catheline S, et al. Shear modulus imaging with 2-D transient elastography [J]. *Ultrasonics, Ferroelectrics and Frequency Control*, 2002, **49**(4): 426 − 435.

[3] Dutt Vinayakal, Kinnick Randall R, Muthupillai Rajaa, et al. Acoustic shear-wave imaging using echo ultrasound compared to magnetic resonance elastography [J]. *Ultrasound in Medicine and Biology*, 2000, **26**(3): 397 − 403.

[4] Ophir J, Cespedes I, Ponnekanti H, et al. A quantitative method for imaging the elasticity of biological tissues [J]. *Ultrasonic Imaging*, 1991, **13**(2): 111 − 134.

[5] O'Donnell M, Skovoroda A R, Shapo B M, et al. Internal displacement and strain imaging using ultrasonic speckle tracking [J]. *Ultrasonics, Ferroelectrics and Frequency Control*, 1994, **41**(3): 314 − 325.

[6] Skovoroda A R, Emelianov S Y, O'Donnell M. Tissue elasticity reconstruction based on ultrasonic displacement and strain images[J]. *Ultrasonics, Ferroelectrics and Frequency Control*, 1995, **42**(4): 747 − 765.

[7] Kallel F, Bertrand M. Tissue elasticity reconstruction using linear perturbation method [J]. *IEEE Transactions on Medical Imaging*, 1996, **15**(3): 299 − 313.

[8] Zhu Yanning, Hall Timothy J, Jiang Jingfeng. A finite-element approach for Young's modulus reconstruction [J]. *IEEE Transactions on Medical Imaging*, 2003, **22**(7): 890 − 901.

[9] Liew Haw Ling, Pinsky Peter M. Recovery of shear modulus in elastography using an djoint method with B-spline representation [J]. *Finite Elements in Analysis and Design*, 2005, **41**(7, 8): 778 − 799.

[10] Jia Ruiyu, Wang Bingquan, Xu Lanbing. The edges extraction of CT images of liver which contain illness [J]. *Journal of Anhui University*(*Natural Science Edition*), 1998, **22**(1): 56 − 59. (in Chinese)

[11] Wu Jian, Ding Hui, Wang Guangzhi, et al. The frequency features and application of edge detection differential operators in medical image [J]. *J Biomed Eng*, 2005, **22**(1): 82 − 85.

[12] Wang He, Zhuang Tiange, Jia Dazong. Extraction of fuzzy boundary in medical images [J]. *Chinese Journal of Biomedical Engineering*, 2001, **20**(2): 138 − 142. (in Chinese)

[13] Wei Chunrong, Zhang Xiaofei, Chen Hongbo, et al. A

method of medical image registration based on contour extraction [J]. *Journal of Guangxi Normal University*, 2003, **21**(2): 33 - 36. (in Chinese)

[14] Eberhart R, Kennedy J. A new optimizer using particle swarm theory [A] In: *Proceedings of the Sixth International Symposium on Micro Machine and Human Science* [C]. Nagova, Japan, 1995. 39 - 43.

[15] Shi Y, Eberhart R. A modified particle swarm optimizer [A]. In: *IEEE World Congress on Computational Intelligence* [C]. Anchorage, Alaska, 1998. 69 - 73.

基于粒子群优化算法的生物组织杨氏模量的重构

陈 敏 王 楠 汤文成

(东南大学机械工程学院,南京 210096)

摘要:为了定量求解生物病变组织的杨氏模量,提出了一种基于边缘提取技术和图像配准技术的杨氏模量反演方法.在已知生物组织边缘位移及病变边缘的基础上,根据力的分布,构造单元系统,运用有限元反演方法(IFEM),计算出组织的杨氏模量.在此基础上估计全局杨氏模量范围,采用改进粒子群优化算法(PSO),计算出生物组织整体的杨氏模量分布.该算法克服了其他杨氏模量重建算法的限制,放松了对位移和边界力的要求.通过多次数值实验得出:算法对存在误差的边缘位移同样有效;改进的 PSO 算法在较大范围内叠代搜索,总能向理论值靠近,并得到可行解.

关键词:杨氏模量;有限元反演法;粒子群优化算法

中图分类号:TH123